

# Polycyclic Aromatic Hydrocarbons Extraction Based on Graphene Coated Magnetic Alloy Nanoparticles

Maria Sarno, Eleonora Ponticorvo<sup>\*</sup>, Claudia Cirillo, Paolo Ciambelli

Department of Industrial Engineering and Centre NANO\_MATES University of Salerno  
Via Giovanni Paolo II, 132 - 84084 Fisciano (SA), Italy  
[eponticorvo@unisa.it](mailto:eponticorvo@unisa.it)

In this paper we reported on a new promising nanosorbent constituted by core-shell few layer graphene coated metal nanoparticles (G-FeCo). It combines the superparamagnetism of the FeCo alloy and the strong adsorption ability of the carbon materials to give a direct excellent absorption efficiency and rapid separation. Two PAHs as model analytes, fluoranthene and anthracene, were determined by the combination of magnetic solid phase extraction (MSPE) and GC-MS analysis. Limits of detection of PAHs were found for analytes solutions in the linear range of 2-200 ng l<sup>-1</sup>. The accuracy of the method was evaluated by the recoveries of spiked samples. Very good recoveries was achieved with G-FeCo. Our results proved that the present approach is sensitive and efficient for the extraction of PAHs traces. This simple method provided a very high extraction efficiency and short analysis times.

## 1. Introduction

PAHs (Polycyclic Aromatic Hydrocarbons) are very difficult to degrade due to their high stability and complex molecular structures and are considered very significant environmental pollutants. The PAHs structural features make them carcinogenic, mutagenic, and teratogenic (Srogi, 2007). There is an increasing interest in the detection of PAHs in environmental water sources for the protection of health and environment. Magnetic Solid-Phase Extraction (MSPE), that is a magnetic based Solid-Phase Extraction (SPE), has gained more and more attention in trace analysis (Liu et al., 2012). To ensure rapid separation high magnetization value are required. Many studies have been focused on magnetite nanoparticles (NPs) (Metaxa et al., 2016; Adamaki et al., 2016; Sarno et al., 2016b). Carbon materials, including activated carbon, graphitized carbon black, porous graphitic carbon and graphene, possesses strong adsorption ability (Sreeprasad et al., 2013). Carbon-encapsulated metal or metal carbide nanocrystallites have been generated by the Kratschmer arc-discharge process already in 1995 (Scott et al., 1995). Since then, many studies have shown that in the presence of metal nanoparticles (Co, Fe, Ni, Cr, Au, etc), graphitized carbon structures, such as carbon nanotubes and carbon onions, are formed under arc-discharge, laser ablation, and electron irradiation (Ang et al., 2004). Gedanken and co-workers reported a sonochemical procedure that leads to air-stable cobalt nanoparticles (Nikitenko et al., 2001). Johnson et al. describe a simple method to prepare carbon-coated magnetic Fe and Fe<sub>3</sub>C nanoparticles by direct pyrolysis of iron stearate at 900 °C under an argon atmosphere (Geng et al., 2004). Moreover, carbon-coated nanoparticles are usually in the metallic state, and thus have a higher magnetic moment than the corresponding oxides. Chemical Vapor Deposition (CVD) technique offers the advantage of being the easiest to scale up towards an economically viable production (Seo et al., 2006). On the other hand, at the best of our knowledge, FeCo NPs covered by graphene have been never tested for this purpose although it is very promising. In this paper, we reported on a new promising nanosorbents constituted by core-shell few layer graphene coated metal NPs (G-FeCo). It combines: (i) the superparamagnetism of the FeCo alloy (a very high saturation magnetization value of 238 e.m.u./g was found in Sarno et al. 2016a (Sarno et al., 2016a)) permitting a faster separation than that previously obtained (Sarno et al., 2016b); and (ii) the strong adsorption ability of graphene, that avoiding further functionalization, allows an excellent absorption efficiency. The stable core-shell G-FeCo NPs were synthesized by catalytic chemical vapor deposition (CCVD) of methane at atmospheric pressure using a catalyst prepared by wet impregnation of gibbsite (γ-

Al(OH)<sub>3</sub> powder with cobalt acetate and iron acetate solutions (Sarno et al., 2014; Sarno et al., 2016a). Raman Spectroscopy, Transmission Electron Microscopy (TEM) and X-ray diffraction (XRD) were employed for characterization. To examine the feasibility of this method, we selected two representative PAHs as model compounds: fluoranthene (Flu) and anthracene (Ant), their determination was carried out by the combination of MSPE and gas chromatography-mass spectroscopy (GC-MS) analysis. Limits of detection of PAHs was found for analytes solutions in the linear range of 2-200 ng l<sup>-1</sup>. The accuracy of the method was evaluated by the recoveries of spiked samples. Our results proved that the present approach is sensitive and efficient for the extraction of trace PAHs. This method provided a very high extraction efficiency and short analysis times.

## 2. Experimental Section

### 2.1 Preparation of G-FeCo nanoparticles

The Co, Fe catalyst (50 wt.% of each metal) was prepared by wet impregnation of gibbsite ( $\gamma$ -Al(OH)<sub>3</sub>) powder (Sarno et al., 2012; Giubileo et al., 2012; Sarno et al., 2014) with cobalt acetate and iron acetate solutions followed by drying at 80°C for 3 h.

CCVD was performed in a continuous flow microreactor fed by a methane–hydrogen gas mixture.

The typical procedure for the preparation of G-FeCo nanoparticles includes (1a) feeding the reacting gas to the analyzers to verify the steady state inlet concentration. (1b) N<sub>2</sub> is fed to the reactor by another feed line to pre-treat the catalyst. (2) The pre-treatment nitrogen flow was stopped using the bypass valve, and the reacting gas stream was started to feed the reactor. (3a) After 5 min, the reacting gas stream was stopped, and nitrogen was fed to the reactor. Next, (3b) the reacting gas was fed to the analyzers. (4) The reactor was extracted from the furnace and allowed to cool under ambient temperature conditions. (5) Chemical attack, in a diluted HF solution 15 vol. % and for 3 h, followed by a centrifugation and washing, in distilled water, under filtration, to separate the G-FeCo from alumina.

Transmission electron microscopy (TEM) images were acquired using a FEI Tecnai electron microscope operated at 200 KV with a LaB<sub>6</sub> filament as the source of electrons. XRD measurements were performed with a Bruker D8 X-ray diffractometer using CuK $\alpha$  radiation. The KBr technique was applied for determining the FT-IR spectra of the samples by using Vertex 70 apparatus (Bruker Corporation). Spectra were recorded the scanning range was from 4000 a 400 cm<sup>-1</sup>.

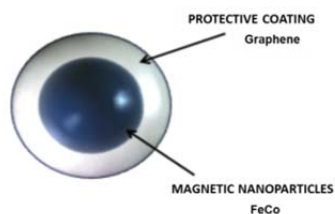


Figure 1: Scheme of core-shell G-FeCo.

### 2.2 Extraction procedure

First of all, 4 mg of G-FeCo NPs were cleaned and activated with acetonitrile and distilled water in sequence. After sample solution preparation (Figure 2-step 1), water was added to the stock solution to get various final concentrations of PAHs over a range of 2 and 200 ng/l (2, 10, 20, 30, 50, 80, 100, 150, 200 ng/l), followed by adding an appropriate amount of G-FeCo NPs (Figure 2-step 2).

A sonication step was performed to promote the adsorption (Figure 2-step 3). The NPs were then separated within few minutes (about 5 min) under an external magnetic field (Figure 2-step 4).

PAHs were eluted from G-FeCo NPs sorbents adding acetonitrile a typical elution solvent (Sarno et al., 2016b) four times followed by a further magnetic separation to recovery NPs, in order to reuse them in subsequent MSPE tests (Figure 2-step 5 and 6).

Finally the eluent was collected and evaporated under a gentle nitrogen flow at ambient temperature (Figure 2-step 7). The eluting solution, about 100 ml, was analysed by gas chromatography.

Determination of PAHs was carried out by gas chromatography-mass spectroscopy (GC-MS, ThermoFisher) analyses. PAHs concentration was analysed by injecting the aliquots of the eluting solution in a gas chromatograph equipped with HP-5 capillary column (0.25 mm $\times$ 0.25 mm $\times$ 30 m). The analysis conditions were set as follows: run time, 40 min; injector temperature, 200 °C; detector temperature, 250 °C. Helium was used

as the carrier gas at a flow rate of 1,2 ml/min. Most appropriate method of operation has been set: the column temperature was kept at 80 °C for 2 min, raised to 185 °C at a rate of 15 °C/min and held for 1 min, then increased to 260 °C at a rate of 10 °C/min and held for 5 min.

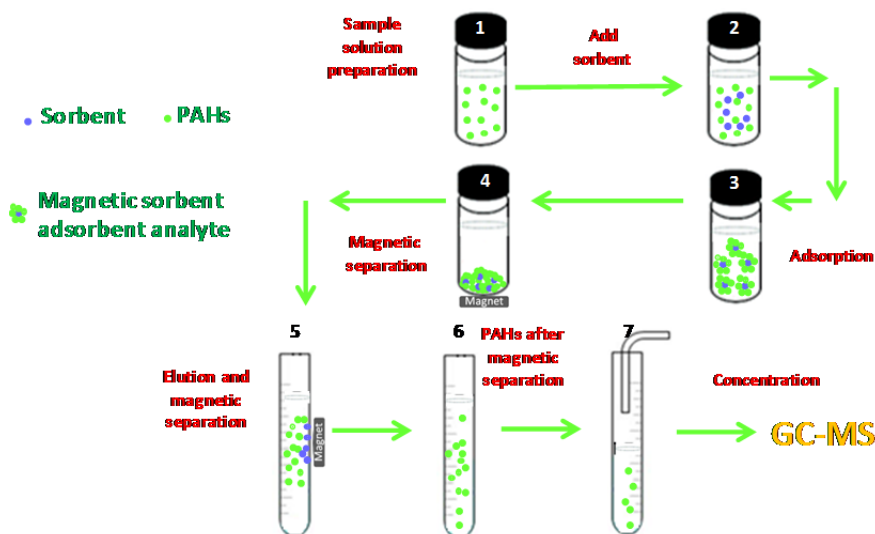


Figure 2: Scheme of the process extraction, showing the different steps as indicated by progressive numbers from 1 to 7.

### 3. Results and discussion

G-FeCo have an average diameter of 4.02 nm, standard deviation 0.84 nm (measured for ~200 nanocrystals), see Figure 3 TEM image. In particular, the nanoparticles are covered by 1-2 layers of graphene, not shown here, see a previous reference (Sarno et al., 2014).

In Figure 4, the X-ray diffraction pattern of G-FeCo is shown. The peaks at  $\sim 45$ ,  $65$  and  $83$   $2\theta$  are typical of a crystalline body-centered-cubic Co/Fe alloy. It is important to note the absence of the diffraction peak at  $\sim 26$   $2\theta$  due to the stacking of the AB graphite. By applying the Scherrer equation to the 110 diffraction peak:  $L_a = 0.9\lambda/B\cos\theta$ , where  $L_a$  is the metal core diameter,  $\lambda$  is the X-ray wavelength,  $B$  is the peak half-maximum width and  $\theta$  is the Bragg angle, the  $L_a$  value was determined to be 4.12 nm, which is very similar to that measured in the HRTEM image.

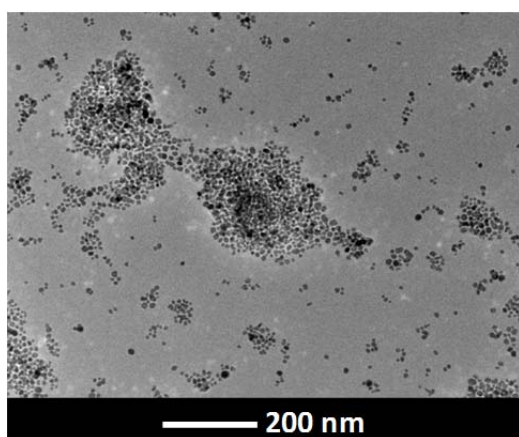


Figure 3. TEM image of G-FeCo nanoparticles.

In Figure 5a, the Raman spectrum of G-FeCo is shown. In particular, the most prominent features (Sarno et al., 2013) of the  $sp^2$  carbon materials, which are known as the G band and the 2D band, were observed at  $1581\text{ cm}^{-1}$  and approximately  $2700\text{ cm}^{-1}$ , respectively, using 514 nm excitation wavelength. A broad 2D band and a pronounced D band, which are characteristic for curved graphene layers (Tan et al., 2004), are

observed. In Figure 6, two photographs of G-FeCo nanoparticles as prepared and in response to Gd magnet are shown. For our G-FeCo nanoparticles, a very high saturation magnetization value of 238 e.m.u./g was found (Sarno et al., 2016a).

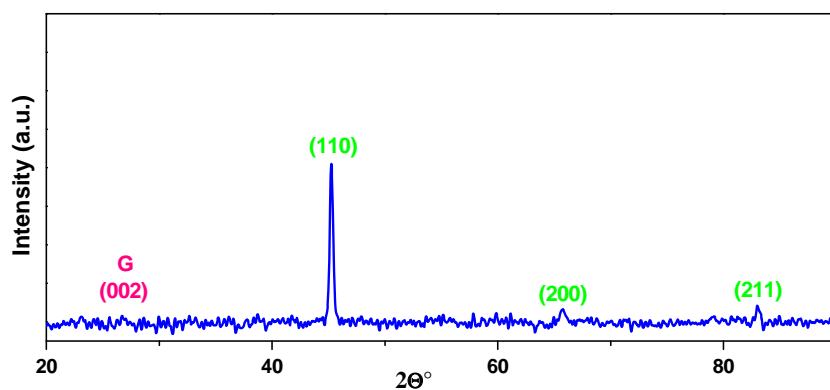


Figure 4. X-ray diffraction pattern of G-FeCo nanoparticles.

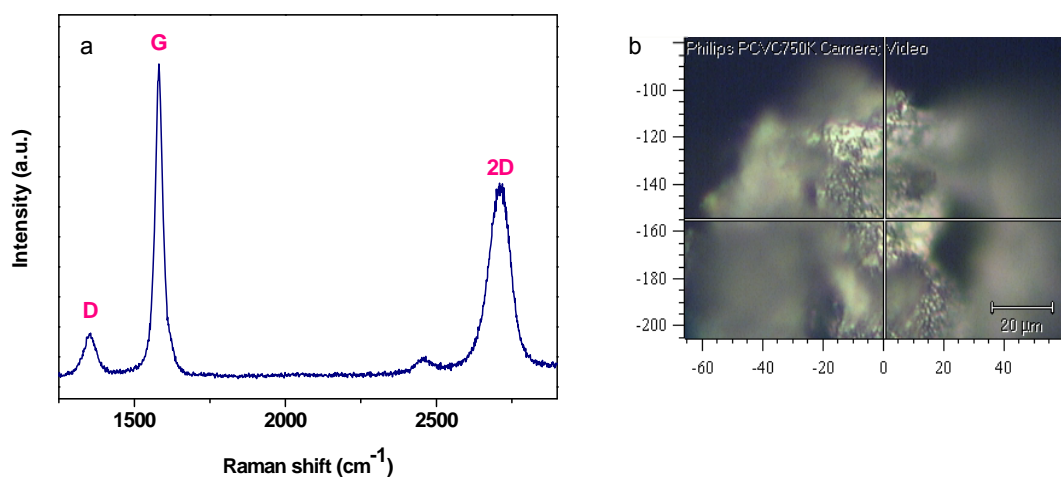


Figure 5. Raman spectrum (a) and optical image at 50X of magnification (b) of G-FeCo nanoparticles.



Figure 6. Photographs of G-FeCo nanoparticles: as prepared (a) and in response to Gd magnet (b).

FT-IR spectroscopy is a useful tool to understand the functional group of any organic molecule. In Figure 7, the infrared spectra of G-FeCo NPs and G-FeCo NPs before elution, and Flu are shown. In the range 1400-

1600  $\text{cm}^{-1}$  vibrational bands from Flu, some up-shifted due to the adsorption on the nanoparticles surface, resulted from the benzene skeleton vibration can be seen in the spectrum of G-FeCo NPs before elution.

To investigate the adsorption of G-FeCo NPs for PAHs, 4 mg of the NPs were added into 200 mL of water solution containing the two PAHs at 200 ng/l level.

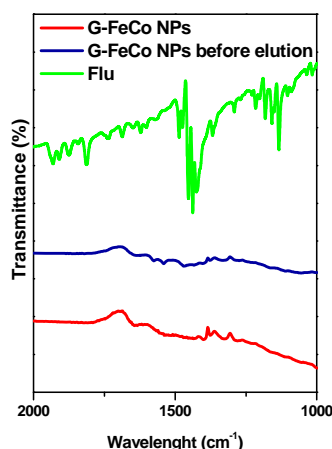


Figure 7. FTIR spectra of G-FeCo NPs and G-FeCo NPs before elution and Flu .

The adsorption amount  $q_a$  expressed as milligrams of adsorbed for grams of G-FeCo adsorbent NPs was calculated according to the Eq(1) :

$$q_a = \frac{V(C_o - C_e)}{m} \quad (1)$$

where  $C_o$  and  $C_e$  represent the initial and final concentrations of the analyte in aqueous solution (mg/l),  $V$  is the volume of the solution (l), and  $m$  is the mass of the adsorbent (g). The values of  $q_a$  for G-FeCo NPs were about 0.01 mg/g for both the analytes.

Finally, we evaluated, with the help of GC-MS linearity range, limit of detection, accuracy and repeatability, the results are shown in Table 1.

Table 1: Analytical parameters of the proposed method.

PAHs	Linear range (ng/l)	Correlation coefficient ( $R^2$ )	LOD (ng/l)	R.S.D. (%)
Ant	2-200	0,99957	0,32	3,8
Flu	2-200	0,99998	0,78	4,5

The LOD was calculated based on the standard deviation of the response and the slope of calibration curve from the following equation (Shrivastava et al., 2011):  $\text{LOD} = 3 \text{ Sb}/m$ ; where  $\text{Sb}$  is the standard deviation of the y-intercept of regression line and  $m$  is the slope of the calibration curve. Good linearity is observed for both analytes throughout the concentration range of 2 to 200  $\text{ng l}^{-1}$ , with  $R^2$  close to 1 in both cases (0.99957 for Ant and 0.99998 for Flu). Additionally, the LOD values for Ant e Flu were 0,32 and 0,78  $\text{ng l}^{-1}$  respectively, showing great sensitivity, the repeatability was calculated by the 3-time determinations of 100  $\text{ng l}^{-1}$  standard sample showing good repeatability. These results indicate that the magnetic adsorbent nanocomposite prepared can enrich the PAHs from water sample efficiently (Sarno et al., 2016b; Bai et al., 2010; Ballesteros-Gómez et al., 2009; Zhang et al., 2010; Zhang et al., 2012; Ding et al., 2010; Liu et al., 2009), in a simple manner and without requiring further functionalization.

#### 4. Conclusion

In this research, core-shell graphene coated G-FeCo magnetic nanoparticles prepared by catalytic chemical vapor deposition on a Co/Fe catalyst in the presence of methane at atmospheric pressure were applied to enrich trace level PAHs from water in a short extraction time. In particular, Magnetic Solid-Phase Extraction (MSPE) was tested for pre-concentration of anthracene (Ant) and fluoranthene (Flu) in water at a trace level. Very low LOD value was found after short MSPE time. The performances of the method indicate that it has a great prospect in pre-concentrating and detecting trace pollutants in real samples.

## References

- Adamaki B., Karatza D., Chianese S., Musmarra D., Metaxa E., Hristoforou E., 2016, Super-paramagnetic nanoparticles: manufacturing, structure, properties, simulation, applications, *Chemical Engineering Transactions*, 47, 79-84, DOI: 10.3303/CET1647014
- Ang K.H., Alexandrou I., Mathur N.D., Amaratunga G.A.J., Haq S., 2004, The effect of carbon encapsulation on the magnetic properties of Ni nanoparticles produced by arc discharge in de-ionized water, *Nanotechnology* 15, 520–524.
- Bai L., Mei B., Guo Q.Z., Shi Z.G., Feng Y.Q., 2010, Magnetic solid-phase extraction of hydrophobic analytes in environmental samples by a surface hydrophilic carbon-ferromagnetic nanocomposite, *J. Chromatogr. A* 1217, 7331–7336.
- Ballesteros-Gómez A., Rubio S., 2009, Hemimicelles of Alkyl Carboxylates Chemisorbed onto Magnetic Nanoparticles: Study and Application to the Extraction of Carcinogenic Polycyclic Aromatic Hydrocarbons in Environmental Water Samples, *Anal. Chem.* 81, 9012–9020.
- Ding J., Gao Q., Luo D., Shi Z.G., Feng Y.Q., 2010, n-Octadecylphosphonic acid grafted mesoporous magnetic nanoparticle: Preparation, characterization, and application in magnetic solid-phase extraction, *J. Chromatogr. A* 1217, 7351–7358.
- Geng J., Jefferson D.A., Johnson B.F.G., 2004, Crystallization, graphite, iron, magnetism, nanostructures, organometallic compounds, particle size, stearates, *Chem. Commun.* 23, 2442–2443.
- Giubileo F., Di Bartolomeo A., Sarno M., Altavilla C., Santandrea S., Ciambelli P., Cucolo A.M., 2012, Field emission properties of as-grown multiwalled carbon nanotube films, *Carbon* 50, 163-169.
- Liu Q., Shi J., Cheng M., Li G., Cao D., Jiang G., 2012, Preparation of graphene-encapsulated magnetic microspheres for protein/peptide enrichment and MALDI-TOF MS analysis, *Chem. Commun.* 48, 1874-1876.
- Liu Y., Li H., Lin J.M., 2009, Magnetic solid-phase extraction based on octadecyl functionalization of monodisperse magnetic ferrite microspheres for the determination of polycyclic aromatic hydrocarbons in aqueous samples coupled with gas chromatography–mass spectrometry, *Talanta* 77, 1037-1042.
- Metaxa E., Berkesi K., Musmarra D., Mamalis A., Hristoforou E., 2016, Synthesis of superparamagnetic nanoparticles for desalination purposes, *Mater. Sci. Forum* 856, 105-115.
- Nikitenko S.I., Koltypin Y., Palchik O., Felner I., Xu X.N., Gedanken A., 2001, Synthesis of highly magnetic, air-stable iron-iron carbide nanocrystalline particles by using power ultrasound, *Angew. Chem.* 113, 4579–4581.
- Sarno M., Cirillo C., Ciambelli P., 2014, Selective graphene covering of monodispersed magnetic nanoparticles, *Chem. Eng. J.* 246, 27-38.
- Sarno M., Cirillo C., Piscitelli R., Ciambelli P., 2013, A study of the key parameters, including the crucial role of H<sub>2</sub> for uniform graphene growth on Ni foil, *J. Mol. Catal. A -Chem.* 366, 303-314.
- Sarno M., Cirillo C., Scudieri C., Polichetti M., Ciambelli P., 2016a, Electrochemical Applications of Magnetic Core-Shell Graphene-Coated FeCo Nanoparticles, *Ind. Eng. Chem. Res.* 55, 3157-3166.
- Sarno M., Ponticorvo E., Cirillo C., Ciambelli P., 2016b, Magnetic Nanoparticles for PAHs Solid Phase Extraction, *Chemical Engineering Transactions*, 47, 313-318, DOI: 10.3303/CET1647053
- Sarno M., Sannino D., Leone C., Ciambelli P., 2012, Evaluating the effects of operating conditions on the quantity, quality and catalyzed growth mechanisms of CNTs, *J. Mol. Catal. A -Chem.* 357, 26-38.
- Scott J.H.J., Majetich S.A., 1995, Morphology, structure, and growth of nanoparticles produced in a carbon arc, *Phys. Rev. B* 52, 12564–12571.
- Seo W.S., Lee J.H., Sun X., Suzuki Y., Mann D., Liu Z., Terashima M., Yang P.C., McConnell M.V., Nishimura D.G., Dai H., 2006, FeCo/graphitic-shell nanocrystals as advanced magnetic-resonance-imaging and near-infrared agents, *Nat. Mater.* 5, 971–976.
- Shrivastava A., Gupta V. B., 2011, Methods for the determination of limit of detection and limit of quantitation of the analytical methods, *Chron. Young Sci.* 2, 21-25.
- Sreeprasada T.S., Gupta S.S., Maliyekkal S.M., Pradeepa T., 2013, Immobilized graphene-based composite from asphalt: Facile synthesis and application in water purification, *J. Hazard Mater.* 246-247, 213-220.
- Srogi K., 2007, Monitoring of environmental exposure to polycyclic aromatic hydrocarbons: a review, *Environ. Chem. Lett.* 5, 169-195.
- Tan P., Dimovski S., Gogotsi Y., 2004, Raman scattering of non-planar graphite: arched edges, polyhedral crystals, whiskers and cones, *Philos. Trans. A Math. Phys. Eng. Sci.* 362, 2289-2310.
- Zhang S.X., Niu H.Y., Cai Y.Q., Shi Y.L., 2010, Barium alginate caged Fe<sub>3</sub>O<sub>4</sub>@C18 magnetic nanoparticles for the pre-concentration of polycyclic aromatic hydrocarbons and phthalate esters from environmental water samples, *Anal. Chim. Acta* 665, 167–175.
- Zhang X., Xie S., Paau M.C., Zheng B., Yuan H., Xiao D., Choi M.M., 2012, Ultrahigh performance liquid chromatographic analysis and magnetic preconcentration of polycyclic aromatic hydrocarbons by Fe<sub>3</sub>O<sub>4</sub>-doped polymeric nanoparticles, *J. Chromatogr. A* 1247, 1–9.